Research Article

Structural and Optical Properties of Spray Coated Carbon Hybrid Materials Applied to Transparent and Flexible Electrodes

Grzegorz Wroblewski,[1] Barbara Swatowska,[2] Wieslaw Powroznik,[2] Malgorzata Jakubowska,[1,3] and Tomasz Stapinski[2]

[1]*Institute of Metrology and Biomedical Engineering, Warsaw University of Technology, A. Boboli St. 8, Warsaw, Poland*
[2]*Department of Electronics, AGH University of Science and Technology, Mickiewicza Av. 30, 30-059 Krakow, Poland*
[3]*CEZAMAT Centre for Advanced Materials and Technologies, Poleczki St. 19, 02-822 Warsaw, Poland*

Correspondence should be addressed to Grzegorz Wroblewski; g.wroblewski@mchtr.pw.edu.pl

Transparent and flexible electrodes were fabricated with cost-effective spray coating technique on polyethylene terephthalate foil substrates. Particularly designed paint compositions contained mixtures of multiwalled carbon nanotubes and graphene platelets to achieve their desired rheology and electrooptical layers parameters. Electrodes were prepared in standard technological conditions without the need of clean rooms or high temperature processing. The sheet resistance and optical transmittance of fabricated layers were tuned with the number of coatings; then the most suitable relation of these parameters was designated through the figure of merit. Optical measurements were performed in the range of wavelengths from 250 to 2500 nm with a spectrophotometer with the integration sphere. Spectral dependence of total and diffusive optical transmission for thin films with graphene platelet covered by multiwalled carbon nanotubes was designated which allowed determining the relative absorbance. Layer parameters such as thickness, refractive index, energy gap, and effective reflectance coefficient show the correlation of electrooptical properties with the technological conditions. Moreover the structural properties of fabricated layers were examined by means of the X-ray diffraction.

1. Introduction

Transparent electrodes are used in a variety of applications such as dye-sensitized solar cells [1, 2], antennas [3, 4], electrodes in displays [5, 6], supercapacitors [7, 8], or heating elements [9]. In most cases transparent electrodes are fabricated with physical and chemical vapour deposition methods (PVD and VCD), which can be used for the deposition of conductive thin metal oxide layers like indium tin oxide (ITO) [10], (AZO) [11], (FTO) [12], (GZO) [13], or (ZnO) [14]. Vacuum techniques are strongly linked with many technological issues like complicated and expensive equipment and problems in providing stable quality of vacuum in larger chambers and high installation and exploitation costs. Moreover conductive oxides are brittle; thus they are not suitable for flexible electronics applications which could be resistant for multicycle bending. Therefore there is a need for large-scale and vacuum-free alternative methods like printing (screen printing [15], inkjet printing [16], flexography [17], gravure [18], or stamp printing [19]), dip coating [20], spin coating [21], or spray coating [22]. The use of these methods needs the development of particular materials and allows the fabrication of new electronic products. New materials need also a deep understanding of properties in aim to establish guidelines for electronic devices design and development.

The use of novel materials like carbon nanomaterials allows the electrodes to be also flexible which was not achievable for metal oxides such as ITO [23, 24]. Present paper is related to two kinds of carbon nanomaterials used as functional phases, graphene platelets (GNP) and multiwalled carbon nanotubes (CNT); since they exhibit high mechanical strength [25–27] and can be used for transparent coatings [28–30], they have great electrical properties [31–34] and exhibit better performance than graphite based coatings

TABLE 1: Prepared paints compositions.

Number	Paint name	CNT, wt%	GNP, wt%	NM solvent, wt%
1	CNT0.1	0.100	0.000	99.900
2	CNT0.099/GNP0.001	0.099	0.001	99.900
3	CNT0.09/GNP0.01	0.09	0.010	99.900
4	GNP0.1	0	0.1	99.900
5	CNT0.05/GNP0.05	0.05	0.05	99.900

which was described in our preliminary results [28]. Transparent electrodes should exhibit possibly the highest optical transmission and the lowest sheet resistance. Unfortunately higher optical transmission usually means higher sheet resistance; thus it is important to find the best match between each other. For this purpose figure of merits (FOM) can be used [35–38]. The method of preparation of transparent conductive layers was spray coating since it is a simple, cost-effective, and clean room free technique. Moreover it is easily implementable in production lines and can be used to coat nonflat large area surfaces.

2. Materials and Methods

To prepare transparent electrodes with spray coating technique special low-viscosity paints (around 1 mPa·s) had to be prepared. As a functional phase two carbon nanomaterials were used, graphene platelets (GNP) and multiwalled carbon nanotubes (CNT), both commercially purchased from Graphene Laboratories Inc. GNP were obtained through the graphene oxide reduction and CNT through the catalytic chemical vapour deposition. Graphene platelets had the platelet size between 2 and 25 μm and 10 nm average thickness. Multiwalled carbon nanotubes had the diameter between 1 and 15 nm and length from 10 to 50 μm.

Carbon nanomaterials were suspended in nitromethane (NM) solvent and homogenized. The homogenization was performed in two steps, firstly for 30 s with higher energy with ultrasonic homogenizer Sonics VCX 750 and secondly for 30 min with lower energy in the ultrasonic bath. The homogenization of paints is crucial for the spray coating process performance and allows achieving higher uniformity of prepared electrodes, which is linked to their lower sheet resistance and higher optical transmission. The final paints compositions are presented in the Table 1.

Transparent electrodes were prepared on a flexible polyethylene terephthalate (PET) transparent substrate. Substrates were cleaned before coating with isopropanol, rinsed with distilled water, and dried in a chamber drier in 80°C for 30 min. The spraying gun was mounted on a *XY* plotter that allows fully controllable motion of the tool in both axes. The spraying gun was supplied by the oil-free air from a special compressing system, to avoid the oil impurities in the layer that could increase the sheet resistance. All samples were cured after layers deposition in a chamber drier in 120°C for 30 min to evaporate the solvent. Figures 1, 2, 3, 4, and 5 present the scanning electron microscope (SEM) pictures of
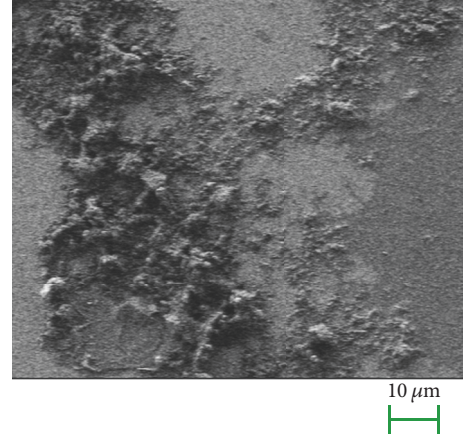

FIGURE 1: SEM picture of sample fabricated with CNT0.1 paint (without graphene platelets).
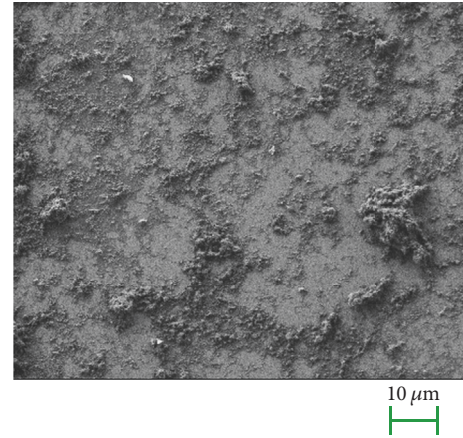

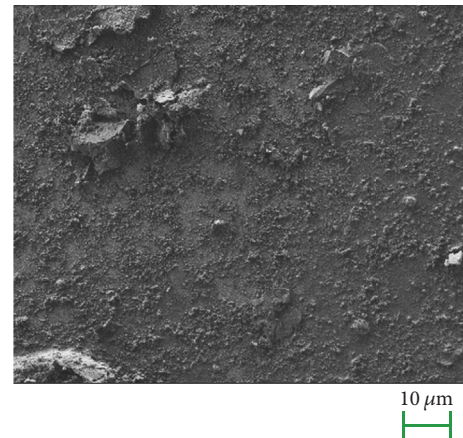FIGURE 2: SEM picture of sample fabricated with CNT0.099/GNP0.001 paint.

FIGURE 3: SEM picture of sample fabricated with CNT0.09/GNP0.01 paint.

samples prepared from paints CNT0.1, CNT0.099/GNP0.001, CNT0.09/GNP0.01, GNP0.1, and CNT0.05/GNP0.05. We can observe that sample with the highest amount of GNP exhibits
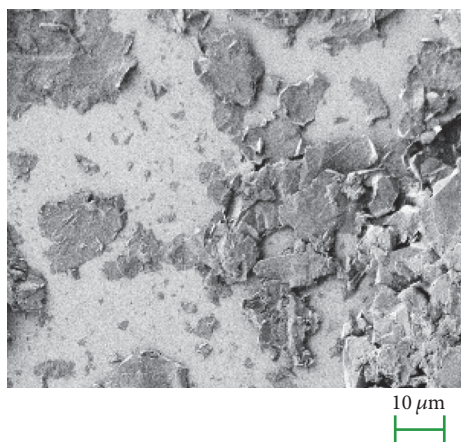
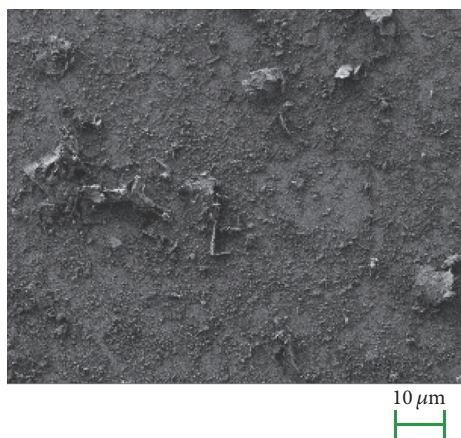Figure 4: SEM picture of sample fabricated with GNP0.1 paint.

Figure 5: SEM picture of sample fabricated with CNT0.05/GNP0.05 paint.

Figure 6: Diffraction patterns of all composites deposited on borosilicate glass.

the lowest amount of CNT agglomerates. In our previous results we have observed that carbon nanotubes are stretched by the graphene platelets along the surface; thus the layer is more homogeneous [39]. Unfortunately in the same time several graphene platelets are not tangential with all their surface to the substrate, which can cause higher roughness and refraction.

The XRD (X-ray diffraction) measurements of samples were performed using Philips X'Pert MPD diffractometer with Cu anode. Diffractograms for samples with multiwalled carbon nanotubes with the addition of graphene platelets on borosilicate glass substrates were measured in the angle range 2θ of 3–80 deg.

The optical measurements of layers with carbon nanotubes and graphene platelets were carried out in the range from 200 to 2500 nm by the use of PERKIN ELMER Lambda 19 spectrophotometer for samples both on a flexible polyethylene terephthalate transparent substrate and on borosilicate glass.

The sheet resistance measurements were made with the use of 4-point probe method with Keithley 2001 in 5 different places of each sample and average value was calculated.
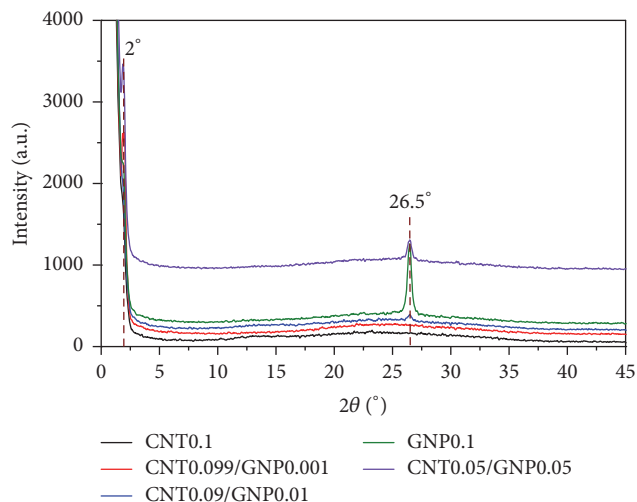
The thickness of the coatings and the surface roughness was measured with a stylus profilometer Veeco Dektak 150 3D. To achieve correct measurements the fraction of 3×0.15 mm of surface of each sample was scanned.

The electrical stability of fabricated samples after several bending cycles was examined with custom made laboratory setup. Sheet resistance of samples was measured in the beginning and after 100, 1,000, 5,000, and 10,000 bending cycles of each sample. The bending radius was 15 mm.

3. Results

Profilometer measurements and sheet resistance where done for 10 samples of each layer material. Profilometer measurements showed that the thickness of prepared samples was quite similar (between 520 nm and 640 nm), but the slight difference between the roughness of the sample with the highest amount of graphene platelets and the other samples was observed. It is caused by the fact that graphene platelets used in the experiment had relatively big diameters, between $2\,\mu$m and $25\,\mu$m, and they usually are not coplanar with their surface to the substrate, what we have described in our previous research [39]. The samples had also similar sheet resistance which is presented in Table 2.

X-ray diffraction measurements allow identifying the structural properties of composite of various graphene platelets contents. The XRD diffractograms of all composites are presented in Figure 6. They reveal two peaks for angle 2θ: at about 2° and 26.5°. The first one is related to (001) graphite oxide, observed also by other authors in graphite oxide material [40]. The second is related to the (002) graphite peak.

In Figure 7, one can see the XRD diffractograms of all samples but with the zoom of areas where characteristic peaks occur. Peak at about 2° does not exist in samples CNT0.1 and CNT0.09/GNP0.01 (Figure 7(a)). The analysis showed differences between the layer of carbon nanotubes with a

TABLE 2: Sheet resistance, thickness, and roughness of prepared samples.

Number	Layer material	Sheet resistance, kΩ/sq	Thickness, μm	Ra, μm
1	CNT0.1	8.6 ± 2.3	0.52 ± 0.11	0.61 ± 0.18
2	CNT0.099/GNP0.001	8.3 ± 2.1	0.55 ± 0.07	0.63 ± 0.09
3	CNT0.09/GNP0.01	8.9 ± 2.4	0.57 ± 0.08	0.81 ± 0.08
4	GNP0.1	11.7 ± 3.1	0.64 ± 0.13	0.92 ± 0.19
5	CNT0.05/GNP0.05	9.4 ± 2.9	0.61 ± 0.09	0.87 ± 0.14
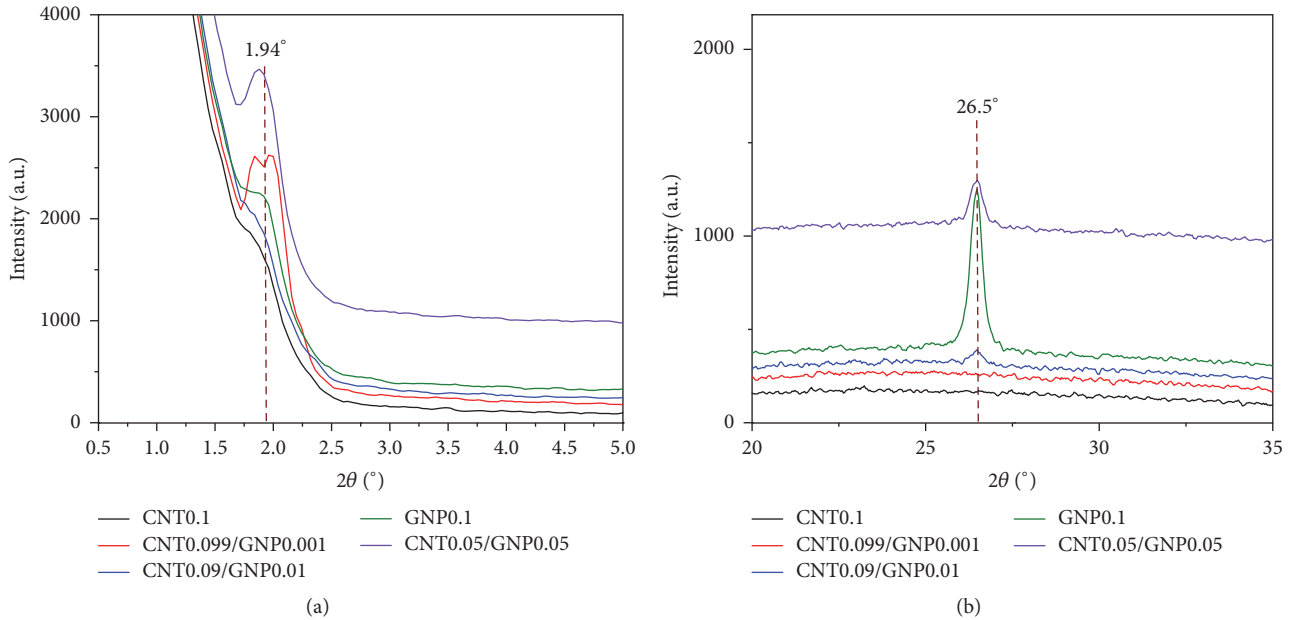
FIGURE 7: Diffraction patterns of samples with various graphene platelets (GNP) and carbon nanotubes (CNT) contents: (a) peak about 2°; (b) peak at 26.5°.

small amount of graphene platelets (CNT0.099/GNP0.001) and a coating with a higher amount of graphene platelets (CNT0.05/GNP0.05). The diffraction pattern of a samples CNT0.099/GNP0.001, CNT0.05/GNP0.05, and GNP0.1 contains (001) graphite oxide peak at about 2° (Figure 7(a)) [41]. This peak may be related to carbon nanotubes as well as to graphene platelets. Additionally the distinct (002) graphite peak for angle 2θ about 26.5° is present in (Figure 7(b)) [42]. The intensity of this peak strongly depends on GNP content in technological mixture. For this reason for layers without graphene platelets (CNT0.1) and with very small GNP content (CNT0.099/GNP0.001) the peak 26.5° does not exist.

Using the Scherrer equation [42] the mean size of grains was calculated (perpendicular to the film surface). From FWHM (full-width at half-maximum) values for (002) graphite diffraction peaks, the obtained D values are in the range from 23 to 25 nm.

The diffraction patterns of base powders reveal no graphite oxide peak at small values of 2-theta (Figure 8). Due to this fact we assume that graphite oxide (in CNT0.099/GNP0.001, CNT0.05/GNP0.05, and GNP0.1)) is formed during samples preparation, for example, during sonication with nitromethane (NM) solvent and CNT.
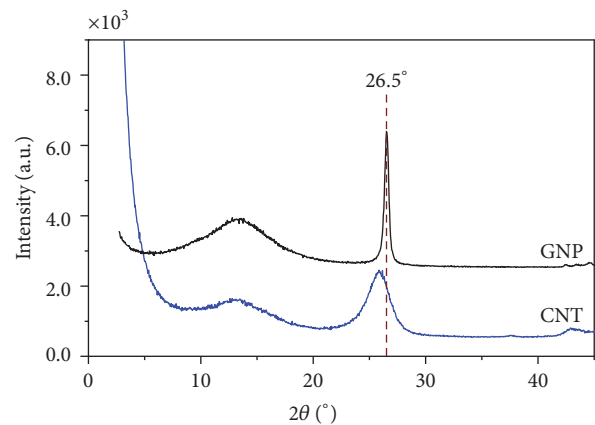

FIGURE 8: Diffraction patterns of powder base materials with carbon nanotubes (CNT) and graphene platelets (GNP).

Figure 9 shows the spectral dependence of total transmittance for flexible PET and how it changes after applying the composite layers with diverse compositions. In visible range the total transmittance decreases from about 85% to 60% for the most transparent composition, which was
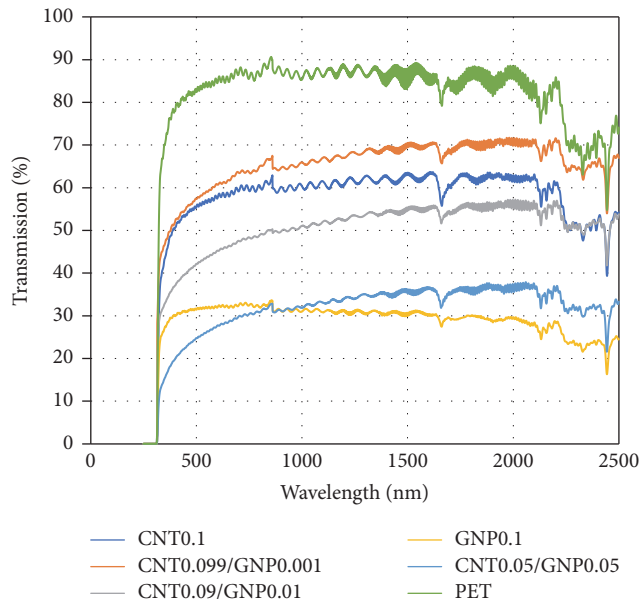
Figure 9: Spectral dependence of the total transmittance for flexible PET substrate and PET with diverse CNT and GNP layers.
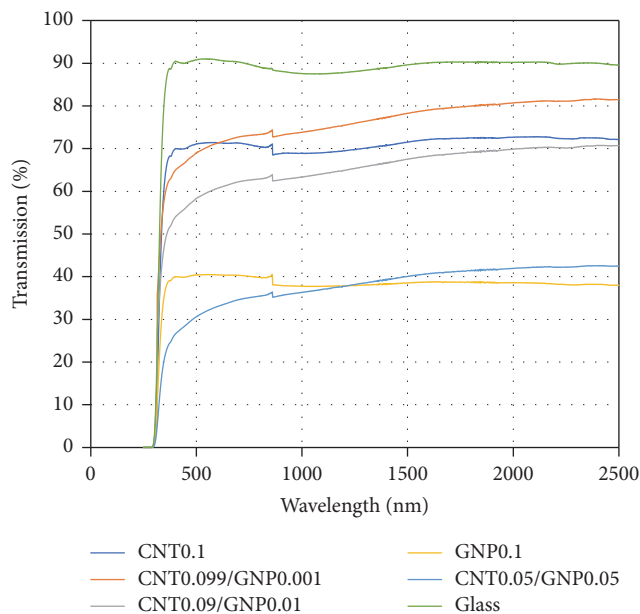

Figure 10: Spectral dependence of the total transmittance for glass substrate and PET with diverse CNT and GNP layers.

Figure 11: Cyclic bending of examined layers made on PET flexible substrate.

the layer with the lowest amount of graphene platelets (CNT0.099/GNP0.001). Both pure CNT and pure GNP and all other hybrid combinations exhibited lower transmission. In the near-infrared between wavelength of 1600 and 2500 nm a significant amount of absorption bands from the substrate was observed. It does not allow a reliable assessment of the optical properties of the material in this spectral range. To provide the reliable measurements in the near IR, samples were also deposited on a glass substrate. The results of total transmission on glass substrates are presented on Figure 10.
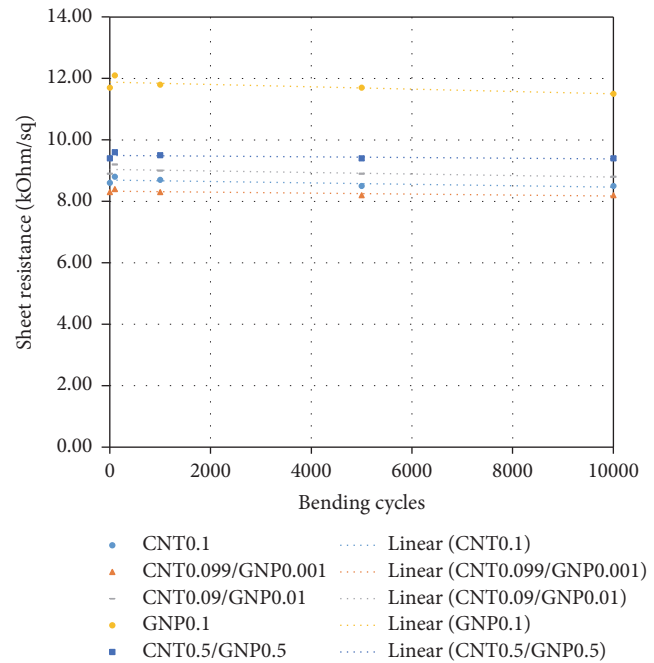
Figure 10 shows similar decrease of transmittance after applying the carbon coatings in the visible wavelengths. Again the composition with the slight adding of graphene platelets exhibited better performance. Figure 10 shows also that the transmission of hybrid materials in the visible spectrum behaves like a logarithmic curve opposite to pure CNT and GNP where it is similar to the curves with right angles. Glass substrate allowed also the observation in the near IR region. It could be seen that the transmission for all hybrid materials is increasing with the wavelengths opposite to pure CNT ang GNP, where after achieving the peak at around 1600 nm is slowly decreasing.

Figure 11 presents the results related to the electrical stability of samples after several bending cycles. All of examined materials exhibited excellent stability regardless the CNT/GNP ratio (sheet resistance changes less than 3.4% in relation). Our results show even a small drop of sheet resistance after 10,000 bending cycles (about 1.8% as regards the value before bending), which is probably caused by the self-arrangement of the carbon nanostructures in the fabricated layers.

4. Conclusions

Carbon nanomaterials consisted of functional phases, graphene platelets (GNP) and multiwalled carbon nanotubes (CNT), which revealed optical properties for applications as transparent coatings of high optical transmission and the low sheet resistance. The analysed layers have a complex structure and a variation of the content of graphene platelets in the structure of layers brings change in the optical properties of material. Spectral dependence of total transmittance in the

TABLE 3: Comparison of hybrid and pure CNT and GNP electrodes on PET.

Number	Paint name	Sheet resistance, kΩ/sq	Transmission at 550 nm, %
1	CNT0.1	8.6 ± 2.3	56 ± 4
2	CNT0.099/GNP0.001	8.3 ± 2.1	60 ± 3
3	CNT0.09/GNP0.01	8.9 ± 2.4	43 ± 2
4	GNP0.1	11.7 ± 3.1	31 ± 5
5	CNT0.05/GNP0.05	9.4 ± 2.9	26 ± 4

middle of visible region (i.e., 550 nm) and sheet resistance for composite layers deposited onto flexible PET were shown in Table 3. It could be seen that the best performance was observed for layers made with CNT0.099/GNP0.001 composition.

X-ray diffractometry indicates the presence of (001) graphite oxide peak (at $2\theta = 2°$) in CNT0.099/GNP0.001, CNT0.05/GNP0.05, and GNP 0.1, strongly associated with the technological process. In graphene platelets reach samples (CNT0.09/GNP0.01, CNT0.05/GNP0.05, and GNP0.1) a characteristic (002) graphite peak at $2\theta = 26.5°$ is observed. The highest intensity is achieved for GNP0.1 sample. This result is in good correlation with optical transmission; sample GNP0.1 has the highest absorption in whole range of wavelength.

Results obtained in this research may be useful for understanding the nature of graphene platelets, carbon nanotubes, and their hybrid compositions in functional composite coatings applicable in optoelectronic devices.

Conflicts of Interest

The authors declare that there are no conflicts of interest regarding the publication of this paper.
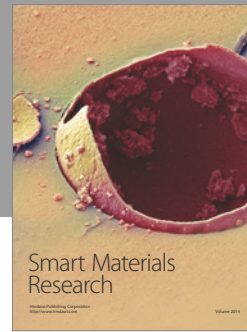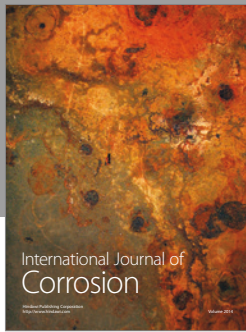
Acknowledgments

References

[1] D. W. Zhang, X. D. Li, H. B. Li et al., "Graphene-based counter electrode for dye-sensitized solar cells," *Carbon*, vol. 49, no. 15, pp. 5382–5388, 2011.

[2] L. Kavan, J.-H. Yum, and M. Grätzel, "Graphene nanoplatelets outperforming platinum as the electrocatalyst in co-bipyridine-mediated dye-sensitized solar cells," *Nano Letters*, vol. 11, no. 12, pp. 5501–5506, 2011.

[3] K.-Y. Shin, J.-Y. Hong, and J. Jang, "Micropatterning of graphene sheets by inkjet printing and its wideband dipole-antenna application," *Advanced Materials*, vol. 23, no. 18, pp. 2113–2118, 2011.

[4] Y.-M. Wu, X. Lv, B. K. Tay, and H. Wang, "Carbon nanotube-based printed antenna for conformal applications," in *Proceedings of the International Conference on Optoelectronics and Microelectronics (ICOM '13)*, pp. 91–93, Harbin, China, September 2013.

[5] M. Sloma, D. Janczak, G. Wroblewski, A. Mlozniak, and M. Jakubowska, "Electroluminescent structures printed on paper and textile elastic substrates," *Circuit World*, vol. 40, no. 1, pp. 13–16, 2014.

[6] G. Jo, M. Choe, S. Lee, W. Park, Y. H. Kahng, and T. Lee, "The application of graphene as electrodes in electrical and optical devices," *Nanotechnology*, vol. 23, no. 11, Article ID 112001, 2012.

[7] K. Jost, D. Stenger, C. R. Perez et al., "Knitted and screen printed carbon-fiber supercapacitors for applications in wearable electronics," *Energy & Environmental Science*, vol. 6, no. 9, pp. 2698–2705, 2013.

[8] M. H. Ervin, L. T. Le, and W. Y. Lee, "Inkjet-Printed Flexible Graphene Based Supercapacitors," *Chemical Engineering Journal*, vol. 89, pp. 1342–1356, 2011.

[9] G. Wróblewski, K. Kielbasinski, B. Swatowska et al., "Carbon nanomaterials dedicated to heating systems," *Circuit World*, vol. 41, no. 3, pp. 102–106, 2015.

[10] Q. Wei, H. Zheng, and Y. Huang, "Direct patterning ITO transparent conductive coatings," *Solar Energy Materials and Solar Cells*, vol. 68, no. 3-4, pp. 383–390, 2001.

[11] M. Sibiński, K. Znajdek, M. Sawczak, and M. Górski, "AZO layers deposited by PLD method as flexible transparent emitter electrodes for solar cells," *Microelectronic Engineering*, vol. 127, pp. 57–60, 2014.

[12] C. Sima, C. Grigoriu, and S. Antohe, "Comparison of the dye-sensitized solar cells performances based on transparent conductive ITO and FTO," *Thin Solid Films*, vol. 519, no. 2, pp. 595–597, 2010.

[13] J.-I. Nomoto, M. Konagai, K. Okada, T. Ito, T. Miyata, and T. Minami, "Comparative study of resistivity characteristics between transparent conducting AZO and GZO thin films for use at high temperatures," *Thin Solid Films*, vol. 518, no. 11, pp. 2937–2940, 2010.

[14] K. Ellmer, A. Klein, and B. Rech, *Transparent conductive zinc oxide: basics and applications in thin film solar cells*, vol. 104, Springer Science & Business Media, 2007.

[15] B. Winther-Jensen and F. C. Krebs, "High-conductivity large-area semi-transparent electrodes for polymer photovoltaics by silk screen printing and vapour-phase deposition," *Solar Energy Materials and Solar Cells*, vol. 90, no. 2, pp. 123–132, 2006.

[16] J.-A. Jeong, J. Lee, H. Kim, H.-K. Kim, and S.-I. Na, "Ink-jet printed transparent electrode using nano-size indium tin oxide particles for organic photovoltaics," *Solar Energy Materials and Solar Cells*, vol. 94, no. 10, pp. 1840–1844, 2010.

[17] M. Hösel and F. C. Krebs, "Large-scale roll-to-roll photonic sintering of flexo printed silver nanoparticle electrodes," *Journal of Materials Chemistry*, vol. 22, no. 31, pp. 15683–15688, 2012.

[18] C.-K. Cho, W.-J. Hwang, K. Eun, S.-H. Choa, S.-I. Na, and H.-K. Kim, "Mechanical flexibility of transparent PEDOT:PSS

electrodes prepared by gravure printing for flexible organic solar cells," *Solar Energy Materials and Solar Cells*, vol. 95, no. 12, pp. 3269–3275, 2011.

[19] C. Lin, X. Zhu, J. Feng et al., "Hydrogen-incorporated TiS$_2$ ultrathin nanosheets with ultrahigh conductivity for stamp-transferrable electrodes," *Journal of the American Chemical Society*, vol. 135, no. 13, pp. 5144–5151, 2013.

[20] C. Terrier, J. P. Chatelon, R. Berjoan, and J. A. Roger, "Sb-doped SnO2 transparent conducting oxide from the sol-gel dip-coating technique," *Thin Solid Films*, vol. 263, no. 1, pp. 37–41, 1995.

[21] J. W. Jo, J. W. Jung, J. U. Lee, and W. H. Jo, "Fabrication of highly conductive and transparent thin films from single-walled carbon nanotubes using a new non-ionic surfactant via spin coating," *ACS Nano*, vol. 4, no. 9, pp. 5382–5388, 2010.

[22] J. G. Tait, B. J. Worfolk, S. A. Maloney et al., "Spray coated high-conductivity PEDOT:PSS transparent electrodes for stretchable and mechanically-robust organic solar cells," *Solar Energy Materials and Solar Cells*, vol. 110, pp. 98–106, 2013.

[23] P. C. Bouten, P. J. Slikkerveer, and Y. Leterrier, "Mechanics of ITO on plastic substrates for flexible displays," *Flat Panel Displays*, 2005.

[24] K. A. Sierros, N. J. Morris, K. Ramji, and D. R. Cairns, "Stress-corrosion cracking of indium tin oxide coated polyethylene terephthalate for flexible optoelectronic devices," *Thin Solid Films*, vol. 517, no. 8, pp. 2590–2595, 2009.

[25] I. W. Frank, D. M. Tanenbaum, A. M. Van der Zande, and P. L. McEuen, "Mechanical properties of suspended graphene sheets," *Journal of Vacuum Science & Technology B: Microelectronics and Nanometer Structures*, vol. 25, no. 6, pp. 2558–2561, 2007.

[26] J.-P. Salvetat, J.-M. Bonard, N. B. Thomson et al., "Mechanical properties of carbon nanotubes," *Applied Physics A: Materials Science and Processing*, vol. 69, no. 3, pp. 255–260, 1999.

[27] J. N. Coleman, U. Khan, W. J. Blau, and Y. K. Gun'ko, "Small but strong: a review of the mechanical properties of carbon nanotube-polymer composites," *Carbon*, vol. 44, no. 9, pp. 1624–1652, 2006.

[28] G. Wróblewskia, M. Słomaa, D. Janczak, A. Młozniakb, and M. Jakubowska, "Influence of carbon nanoparticles morphology on physical properties of polymer composites," *Acta Physica Polonica A*, vol. 125, no. 4, pp. 861–863, 2014.

[29] M. Layani, A. Kamyshny, and S. Magdassi, "Transparent conductors composed of nanomaterials," *Nanoscale*, vol. 6, no. 11, pp. 5581–5591, 2014.

[30] Z. C. Wu, Z. H. Chen, X. Du et al., "Transparent, conductive carbon nanotube films," *Science*, vol. 305, no. 5688, pp. 1273–1276, 2004.

[31] T. Ando, "The electronic properties of graphene and carbon nanotubes," *NPG Asia Materials*, vol. 1, no. 1, pp. 17–21, 2009.

[32] Z. Spitalsky, D. Tasis, K. Papagelis, and C. Galiotis, "Carbon nanotube-polymer composites: chemistry, processing, mechanical and electrical properties," *Progress in Polymer Science*, vol. 35, no. 3, pp. 357–401, 2010.

[33] M. F. L. de Volder, S. H. Tawfick, R. H. Baughman, and A. J. Hart, "Carbon nanotubes: present and future commercial applications," *Science*, vol. 339, no. 6119, pp. 535–539, 2013.

[34] R. Saito, M. Dresselhaus, and G. Dresselhaus, *Carbon nanotubes: synthesis, structure, properties, and applications*, Imperial College Press, 2003.

[35] S. B. Sepulveda-Mora and S. G. Cloutier, "Figures of merit for high-performance transparent electrodes using dip-coated silver nanowire networks," *Journal of Nanomaterials*, vol. 2012, Article ID 286104, 7 pages, 2012.

[36] G. Haacke, "New figure of merit for transparent conductors," *Journal of Applied Physics*, vol. 47, no. 9, pp. 4086–4089, 1976.

[37] D. S. Ghosh, T. L. Chen, and V. Pruneri, "High figure-of-merit ultrathin metal transparent electrodes incorporating a conductive grid," *Applied Physics Letters*, vol. 96, no. 4, Article ID 041109, 2010.

[38] R. G. Gordon, "Criteria for choosing transparent conductors," *MRS Bulletin*, vol. 25, no. 8, pp. 52–57, 2000.

[39] G. Wroblewski, K. Kielbasinski, T. Stapinski et al., "Graphene platelets as morphology tailoring additive in carbon nanotube transparent and flexible electrodes for heating applications," *Journal of Nanomaterials*, vol. 2015, Article ID 316315, 8 pages, 2015.

[40] T. N. Blanton and D. Majumdar, "X-ray diffraction characterization of polymer intercalated graphite oxide," *Powder Diffraction*, vol. 27, no. 2, pp. 104–107, 2012.

[41] J. W. Jang, B. G. Min, J. H. Yeum, and Y. G. Jeong, "Structures and physical properties of graphene/PVDF nanocomposite films prepared by solution-mixing and melt-compression," *Fibers and Polymers*, vol. 14, no. 8, pp. 1332–1338, 2013.

[42] J. I. Langford and A. J. Wilson, "Scherrer after sixty years: a survey and some new results in the determination of crystallite size," *Journal of Applied Crystallography*, vol. 11, no. 2, pp. 102–113, 1978.